(This is a sample cover image for this issue. The actual cover is not yet available at this time.)

Earth and Planetary Science Letters 363 (2013) 192–203

Contents lists available at SciVerse ScienceDirect

Earth and Planetary Science Letters

journal homepage: www.elsevier.com/locate/epsl

Biological Fe oxidation controlled deposition of banded iron formation in the ca. 3770 Ma Isua Supracrustal Belt (West Greenland)

Andrew D. Czaja [a,b,*], Clark M. Johnson [a,b], Brian L. Beard [a,b], Eric E. Roden [a,b], Weiqiang Li [a,b], Stephen Moorbath [c]

[a] Department of Geoscience, 1215 W. Dayton Street, University of Wisconsin, Madison, WI 53706, USA
[b] NASA Astrobiology Institute, University of Wisconsin, Madison, WI, USA
[c] Department of Earth Sciences, University of Oxford, Oxford OX1 3PR, GBR, UK

ARTICLE INFO

Article history:
Received 18 October 2012
Received in revised form
17 December 2012
Accepted 18 December 2012
Editor: T.M. Harrison

Keywords:
Isua Supracrustal Belt
Fe isotopes
femtosecond laser-ablation
anoxygenic phototrophs
Fe oxidation
Early Archean

ABSTRACT

The redox balance of the Archean atmosphere–ocean system is among the most significant uncertainties in our understanding of the earliest history of Earth's surface zone. Most workers agree that oxygen did not constitute a significant proportion of the atmosphere until after ca. 2.45 Ga, after the Great Oxidation Event, but there is less agreement on when O_2 production began, and how this may have been consumed by reduced species such as Fe(II) in the oceans. The Fe redox cycle through time has been traced using banded iron formations (BIFs), and Fe isotopes are increasingly used to constrain the conditions of Earth's paleoenvironments, including the pathways of formation of BIFs. Iron isotope analyses of BIFs from the 3.7 to 3.8 Ga Isua Supracrustal Belt (ISB), obtained by micro-sampling of magnetite-rich layers and conventional analysis, as well as by *in situ* femtosecond laser ablation (fs-LA-ICP-MS), indicate a consistently narrow range of non-zero δ^{56}Fe values. Analysis of magnetite by fs-LA-ICP-MS allows for precise and accurate micron-scale analyses without the problems of orientation effects that are associated with secondary ion mass spectrometry (SIMS) analyses. Magnetite δ^{56}Fe values range from +0.4‰ to +1.1‰ among different bands, but within individual layers magnetite grains are mostly homogeneous. Although these BIFs have been metamorphosed to amphibolite-facies, the metamorphism can neither explain the range in Fe isotope compositions across bands, nor that between hand samples. The isotopic compositions therefore reflect "primary", low-temperature sedimentary values. The positive δ^{56}Fe values measured from the ISB magnetites are best explained by deposition of Fe(III)-oxides produced by partial oxidation of Fe(II)-rich ocean water. A dispersion/reaction model, which accounts for rates of hydrothermal $Fe(II)_{aq}$ input, rates of oxidation, and rates of $Fe(OH)_3$ settling suggests exceptionally low O_2 contents, $<0.001\%$ of modern O_2 contents in the photic zone. Such low levels suggest an anoxygenic pathway is more likely, and the data can be well modeled by anoxygenic photosynthetic Fe(II) oxidation. Comparison of the Fe isotope data from the Isua BIFs with those from the 2.5 Ga BIFs from the Hamersley and Transvaal basins (Australia and South Africa, respectively) suggests a striking difference in Fe sources and pathways. The 2.5 Ga magnetite facies BIFs of Australia and South Africa have δ^{56}Fe values that range from −1.2‰ to +1.2‰ over small scales, and are on average close to 0‰, which is significantly lower than those reported here from the Isua BIFs. The wide range in Fe isotope compositions for the Hamersley and Transvaal BIFs, in concert with C and O isotope data, have been interpreted to reflect bacterial dissimilatory Fe(III) reduction (DIR). The absence of low δ^{56}Fe values in the Isua BIFs, as well as the lack of fine-scale isotopic heterogeneity, may indicate formation prior to widespread DIR.

1. Introduction

The timing and extent of surface oxidation remains one of the outstanding questions in the evolution of the Earth. Although most workers agree that atmospheric O_2 contents were low in the Early Archean (e.g., Holland, 1984; Farquhar et al., 2000), there is increasing evidence for at least some oxygen production prior to the Great Oxidation Event (GOE) at ca. 2.45 Ga based on geochemical and biomarker evidence (e.g., Brocks et al., 1999; Anbar et al., 2007; Kaufman et al., 2007; Eigenbrode et al., 2008; Waldbauer et al., 2009; Kendall et al., 2010; Czaja et al., 2012; Stüeken et al., 2012). From the 3.7 to 3.8 Ga Isua Supracrustal Belt, which contains some of the oldest known metasediments,

* Corresponding author. Present address: Departments of Geology and Chemistry, PO Box 210013, University of Cincinnati, Cincinnati, OH 45221-0013, USA. Tel.: +1 513 556 3574; fax: +1 513 556 6931.
E-mail address: andrew.czaja@uc.edu (A.D. Czaja).

0012-821X/$ - see front matter © 2013 Elsevier B.V. All rights reserved.
http://dx.doi.org/10.1016/j.epsl.2012.12.025

C isotope compositions have been used to infer evidence for biological carbon fixation (e.g., Schidlowski et al., 1979) and possibly for oxygenic photosynthesis (e.g., Rosing, 1999). This interpretation of oxygenic photosynthesis was later supported by studies of U–Th–Pb isotopes that suggested the presence of free oxygen (Rosing and Frei, 2004). It remains unclear, however, what the balance was between oxygen that may have been produced in the Early Archean and its consumption by reduced sinks. Widespread oxygenation of the Earth's surface as early as 3.5 Ga has been suggested based on the presence of allegedly primary Fe(III) minerals (Hoashi et al., 2009; Kato et al., 2009), suggesting that reduced sinks were limited by this time, although recent work has suggested that these Fe(III) minerals are the result of Phanerozoic oxidation (Li et al., 2012).

Banded iron formations (BIFs) represent periods of large-scale interaction between reduced and oxidized iron reservoirs. It is generally accepted that BIF deposition involves upwelling of Fe(II)-rich hydrothermal fluids into shallow waters, followed by oxidation, although the mechanism of oxidation is unclear and may have varied at different times on Earth (e.g., Konhauser et al., 2002; Trendall, 2002; Kappler et al., 2005; Klein, 2005). Rare earth element (REE) patterns for BIFs, including those at Isua (Dymek and Klein, 1988; Klein, 2005; Polat and Frei, 2005), suggest that Fe was sourced to marine hydrothermal fluids, and Si isotopes suggest a hydrothermal source for some of the silica (André et al., 2006; Heck et al., 2011). Oxidation of $Fe(II)_{aq}$ during the Archean to form Fe(III) (oxy)hydroxides, the precursors of BIF oxides, could have been caused by interaction with free O_2 sourced to oxygenic photosynthesis (e.g., Cloud, 1968), anoxygenic photosynthetic Fe(II) oxidation (e.g., Widdel et al., 1993; Kappler et al., 2005), or UV photooxidation (Braterman et al., 1983). All three mechanisms include oxidation of hydrothermal $Fe(II)_{aq}$–$Fe(III)_{aq}$, followed by precipitation of Fe(III) as $Fe(OH)_3$ (Dymek and Klein, 1988; Klein, 2005). Recent experimental studies of UV photooxidation of $Fe(II)_{aq}$ in solutions that are analogous to seawater suggest that this mechanism is unlikely to have been as significant a source of Fe oxides in the Early Archean (Konhauser et al., 2007). The biological processes are feasible means to produce significant Fe(III) oxides (Kappler et al., 2005), and in terms of Fe isotope fractionations, photosynthetic Fe(II) oxidation, or Fe(II) oxidation coupled to nitrate reduction, will produce $Fe(OH)_3$ that has $\delta^{56}Fe$ values up to 3‰ higher than the initial $Fe(II)_{aq}$ under conditions of partial oxidation (Croal et al., 2004; Kappler et al., 2010).

The Isua Supracrustal Belt of southern West Greenland, whose oldest rocks are 3.7–3.8 Ga, include the oldest accepted BIFs (Appel et al., 1998a, 1998b; Fedo et al., 2001; Myers, 2001), and therefore provide insight into Fe cycling in the early Earth. The great antiquity of the Isua BIFs has generated interest in applying new isotope systems for tracing biogeochemical cycling throughout Earth's history. Iron isotope analyses are one such useful approach (e.g., Johnson et al., 2003, 2008a; Rouxel et al., 2005; Yamaguchi et al., 2005; Johnson and Beard, 2006; Planavsky et al., 2009; Czaja et al., 2010, 2012; Heimann et al., 2010; Craddock and Dauphas, 2011), because minerals or fluids that contain ferric Fe tend to have high $^{56}Fe/^{54}Fe$ ratios, whereas ferrous Fe tends to have low $^{56}Fe/^{54}Fe$ ratios. Dauphas et al. (2004, 2007b) and Whitehouse and Fedo (2007) report generally positive $\delta^{56}Fe$ values for magnetite-bearing BIFs from Isua, or ferruginous quartz-pyroxene schists from nearby Akilia Island. Dauphas et al. (2004) suggest that the positive $\delta^{56}Fe$ values indicate that the rocks were produced by low-temperature processes involving transport, oxidation, and precipitation of Fe. These authors did not consider possible metamorphic effects on Fe isotope compositions, but in subsequent papers argued that the consistent $\delta^{56}Fe$ values measured for bulk rocks at Isua, as well as a BIF locality in the Nuvvuagittuq Supracrustal Belt, Canada, suggests that metamorphism did not affect the bulk Fe isotope compositions (Dauphas and Rouxel, 2006; Dauphas et al., 2007a). Whitehouse and Fedo (2007), using secondary ion mass spectrometry (SIMS), found an exceptionally large range in the $\delta^{56}Fe$ values for magnetite at Isua, ~3‰ over a distance of tens of microns, and they

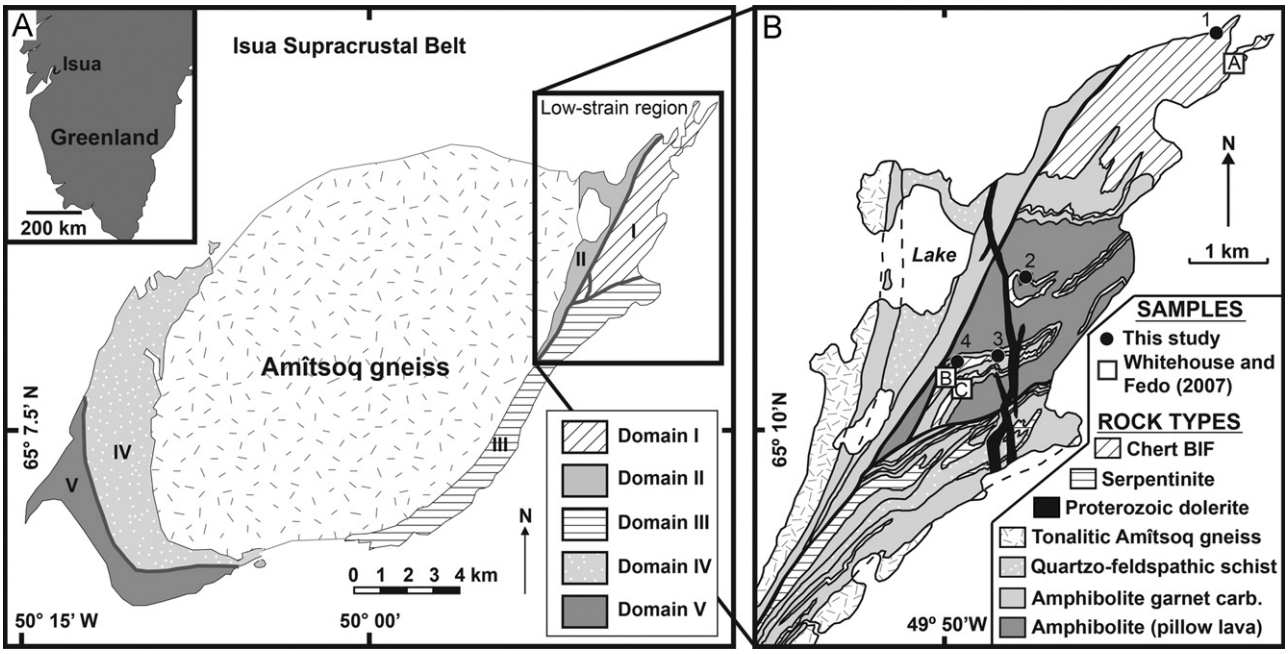

Fig. 1. Location of the Isua Supracrustal Belt in southern West Greenland (A) Simplified geologic map modified from Rollinson (2002, 2003). Domain I is an area of low-strain from which the samples studied here were collected. (B) Geologic map of the low-strain zone indicated by the rectangle in the northwest part of A (modified from Myers, 2001). The black circles indicate the locations where the samples studied here were collected (1=SM/GR/99/10, SM/GR/99/4, SM/GR/93/42, and ID-21-3; 2=IS-626-7A; 3=IS-625-8C; 4=SM/GR/99/21). The open squares indicate the locations where the samples of Whitehouse and Fedo (2007) were collected (A=IS-02-08; B=IS-02-05; C=IS-02-06). Samples SM/GR/93/42, SM/GR/99/4, SM/GR/99/10, and SM/GR/99/21 were collected by Stephen Moorbath. Samples ID-21-3, IS-625-8C, and IS-626-7A were described by Dymek and Klein (1988).

interpret this to indicate that Fe isotope compositions were not reset by metamorphism. It is now recognized, however, that stable isotope measurements by SIMS may be compromised by significant crystal orientation effects for certain minerals, including magnetite (Huberty et al., 2010; Kita et al., 2011). It is therefore possible that the early SIMS data for magnetite at Isua, at least in part, reflect instrumental artifacts.

Here Fe isotope data from BIFs of the Isua Supracrustal Belt are reported, which were collected at millimeter and micrometer scales, via conventional approaches involving micro-drilling and ion-exchange chromatography, as well as femtosecond laser ablation (fs-LA-ICP-MS), respectively. Importantly, *in situ* Fe isotope analysis by fs-LA-ICP-MS is not subject to the crystal orientation effects that can be problematic with SIMS analyses, and therefore offers an opportunity to evaluate the proposal of large, fine-scale Fe isotope heterogeneity in the Isua BIFs. These data suggest that Fe cycling in the early Earth was distinct from that involved in younger BIFs, indicating that temporal changes occurred in the Fe biogeochemical cycle over Earth's history. The data are used here, along with a dispersion/reaction model, to constrain the Fe pathways that occurred during BIF deposition, including an assessment of the relative roles of oxidative drivers and reduced sinks at 3.8 Ga.

2. Materials and methods

2.1. Geologic setting

The 3.7–3.8 Ga Isua Supracrustal Belt (ISB) of southern West Greenland is one of the oldest known successions of volcanic and sedimentary rocks (Moorbath et al., 1973; Appel et al., 1998b). The ISB rocks form an arcuate belt approximately 35 km long and up to 2.5 km wide (Fig. 1), the geology of which has been described previously (e.g., Nutman, 1984; Nutman et al., 1984; Nutman and Bridgwater, 1986; Appel et al., 1998b; Fedo et al., 2001; Crowley et al., 2002). The major rock units that comprise the ISB are shown in Fig. 1B, including a major BIF unit found at Isukasia (Appel et al., 1998a). These rocks are interpreted to have

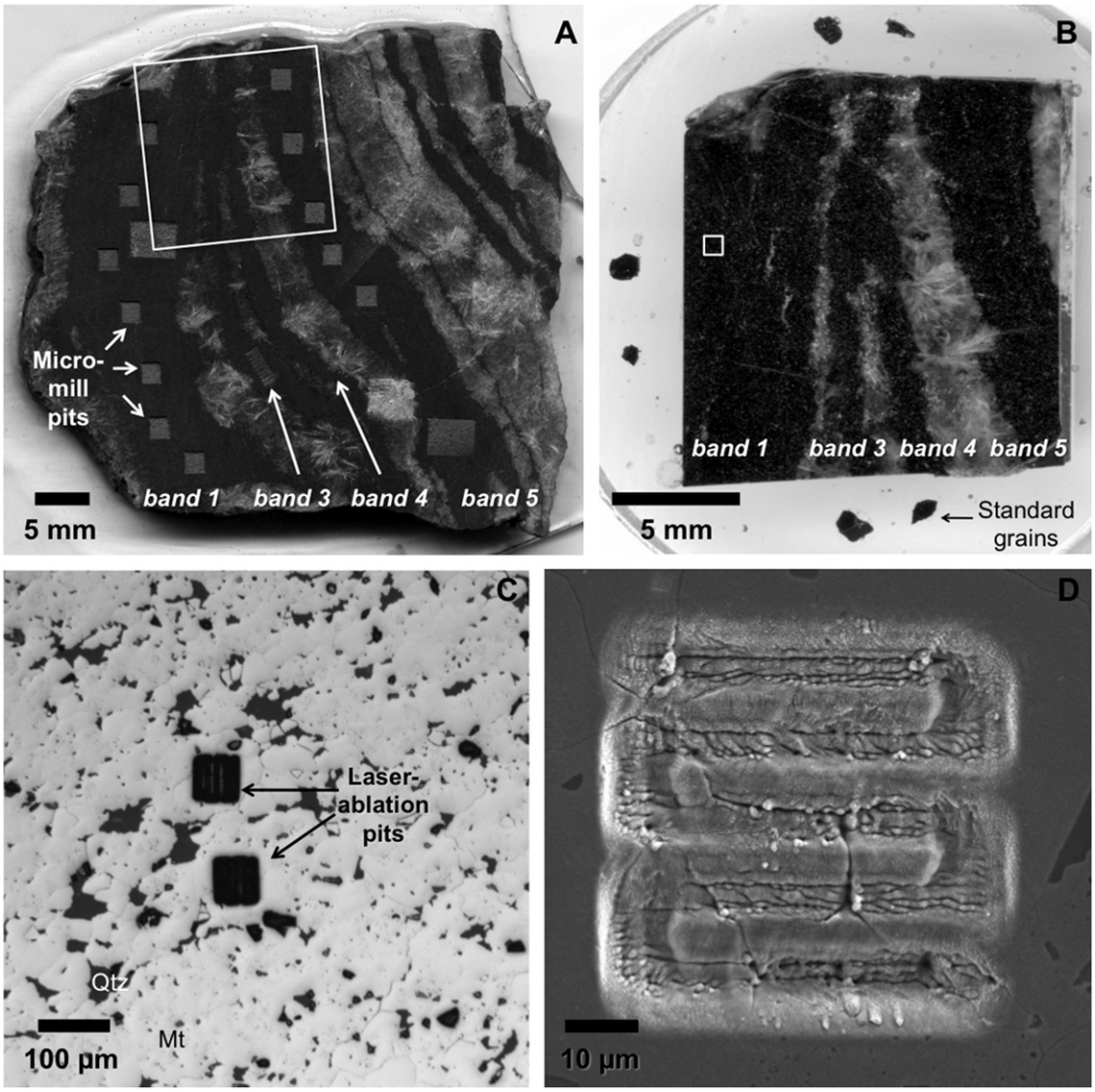

Fig. 2. Representative sample to illustrate the scales of isotope analyses. (A) Slab of sample SM/GR/93/42 from which micro-milled samples were collected (three pits are indicated; light gray pits along dark gray magnetite bands). This sample includes four bands from which Fe isotopes were analyzed, either by conventional means or laser-ablation. The white square indicates the portion cut for mounting in a 1-inch epoxy round for laser-ablation analyses. (B) Image of 1-inch round epoxy plug containing a portion of sample SM/GR/93/42 as well as grains of our in-house magnetite standard, 08-BI-12. The white square indicates the region imaged in part C. (C) High magnification reflected light image of a magnetite band showing two laser ablation pits. The presence of quartz (qtz, dark gray) and magnetite (mt, light gray) are indicated. (D) SEM image of a representative laser ablation pit from sample SM/GR/93/42. See Electronic Annex Fig. EA1 for images of all samples.

been deposited in water ≤ 200 m (Fedo et al., 2001), and have been subjected to amphibolite-facies metamorphism (Boak and Dymek, 1982; Rosing et al., 1996; Rollinson, 2002, 2003; Heijlen et al., 2006). The eastern portion of the Isua Supracrustal Belt is a region of low strain and as such, metamorphic recrystallization is likely to be minimal there (Fig. 1A). This region includes three tectonic domains: Domain I, Domain II, and the northeast portion of Domain III (Rollinson, 2002, 2003). Domain I is interpreted to be the region of least strain in the belt where primary depositional features are still recognizable (Appel et al., 1998a, 1998b; Fedo et al., 2001; Myers, 2001; Rollinson, 2002, 2003), and is the region from which the samples studied here come (Fig. 1B).

2.2. Samples

The seven specimens of Isua BIFs used in this study (Electronic Annex Fig. EA1) were examined and imaged by secondary electron microscopy (SEM; Hitachi S-3400) and analyzed by energy-dispersive X-ray spectroscopy (EDS) to document areas of pure magnetite, free of significant silicate contamination (e.g., Fig. 2). Major-element compositions for magnetite grains from representative samples were determined by wavelength-dispersive spectroscopy (WDS; CAMECA SX51 electron microprobe). The electron microprobe was operated at 15 keV and 20 nA of Faraday cup current in a fixed spot mode with a focused beam. Natural magnetite was used as a standard. Data were reduced based on the stoichiometry of oxygen for magnetite (4).

The iron isotope compositions of multiple individual magnetite layers from the seven BIF specimens were investigated on two spatial scales. Areas of approximately 2 mm by 2 mm by 0.1 mm deep from all seven specimens were sampled using a Merchantek micro-mill (Figs. 2EA1; Herrick, 2007). Sampling at a much smaller scale was done using femtosecond laser-ablation, over areas of approximately 60 μm by 60 μm by 5 μm deep for five of the seven specimens (Figs. 2, EA1 and EA2). Iron isotope data are reported here in standard delta notation as both δ^{56}Fe and δ^{57}Fe, both in units of per mil (‰):

$$\delta^{5x}\mathrm{Fe} = [(^{5x}\mathrm{Fe}/^{54}\mathrm{Fe})_{\mathrm{sample}}/(^{5x}\mathrm{Fe}/^{54}\mathrm{Fe})_{\mathrm{std}} - 1] \times 10^3 \quad (1)$$

for which x is either 6 or 7 and the reference ratio is the average of igneous rocks (Beard et al., 2003). The δ^{56}Fe value of the IRMM-014 standard is -0.09‰ on this scale (Beard and Johnson, 2004). All isotopic analyses were performed using a Micromass *IsoProbe* MC-ICP-MS.

Conventional Fe isotope analysis was performed on powders obtained by micro-milling (MM; Herrick, 2007). Samples were dissolved in heated Savillex beakers using concentrated HF and HNO_3 for 24 h, dried down, and subsequently re-suspended in 8 M HCl and heated for another 24 h. This process was repeated until the samples were completely dissolved. Iron was then separated for conventional mass analysis using anion-exchange chromatography as described previously (Beard and Johnson, 1999; Beard et al., 2003). Isotopic analysis was done using an Aridus desolvating nebulizer, following the methods of Beard et al. (2003) and Albarède et al. (2004). Analytical precision and accuracy was determined by multiple analyses of samples, including multiple analyses of the same solution, as well as duplicate processing through ion-exchange columns. Multiple analyses of the same sample solution and analyses of multiple aliquots of a single sample yield a 2-σ error in δ^{56}Fe values of ± 0.07‰ ($n=66$) for the average of replicates for the conventional isotopic analyses (Herrick, 2007).

Femtosecond laser ablation (fs-LA) analyses were performed using a Photon Machines Analyte-fs that was operated at either 198 nm or 266 nm, with a pulse width of 200 fs. Samples were ablated with a fluence of ~ 1 J cm^{-2} in a small-volume laminar flow cell that was flushed with He as a carrier gas at a rate of 0.5 L min^{-1}. The carrier gas stream was combined with 0.5 L min^{-1} Ar and 6–8 mL min^{-1} N_2 streams in a quartz mixing cell prior to introduction to the MC-ICP-MS. Typically, a volume of $\sim 1.8 \times 10^4$ μm^3 was ablated for each isotopic analysis (see Figs. EA1 and EA2). Samples were bracketed with analyses of an in-house magnetite standard (08-BI-12). This standard has a homogeneous δ^{56}Fe value of 0.32 ± 0.06‰ (2-σ), as determined by conventional MC-ICP-MS; laser ablation analyses produce an average δ^{56}Fe value of 0.31 ± 0.24‰ (2-σ) (Table EA3).

3. Results

The compositions of magnetite studied here as determined by WDS are homogeneous near-pure end member Fe_3O_4, and contain only minor Al_2O_3 substitution of < 0.15 wt% (Electronic Annex Table EA1; Herrick, 2007). All other oxides, including TiO_2, SiO_2, MgO, MnO, CaO, Na_2O, and K_2O, occur in negligible quantities (≤ 0.06 wt%).

The total range of magnetite δ^{56}Fe values ($\delta^{56}Fe_{Mt}$) for the samples collected by micromill is $+0.46$‰ to $+1.17$‰ and the range for the averages of multiple analyses of individual samples is $+0.48$‰ to $+1.11$‰ (Table EA2, Figs. 3, EA1 and EA3; Herrick, 2007). It is important to note that these ranges span multiple samples collected kilometers apart and there is no apparent trend in δ^{56}Fe values of the Isua BIFs across the geographic range sampled (compare Figs. 1 and 3). Individual samples are much more homogeneous and have a range in δ^{56}Fe values of less than < 0.13‰ within individual bands (Table EA2 and Fig. 3). Three samples have small ranges in $\delta^{56}Fe_{Mt}$ values that lie outside analytical uncertainties. Band 4 of SM/GR/99/4 has δ^{56}Fe values that range from 0.61‰ to 0.79‰ with a 2-σ error of 0.14‰ (Table EA2). Band 4 of sample SM/GR/99/21 has $\delta^{56}Fe_{Mt}$ values that range from 0.83‰ to 1.09‰ with a 2-σ error of 0.17‰ (Table EA2). Band 1 of sample SM/GR/93/42 has somewhat heterogeneous $\delta^{56}Fe_{Mt}$ values, ranging from 0.93‰ to 1.17‰ with a 2-σ error of 0.13‰ (Table EA2).

The $\delta^{56}Fe_{Mt}$ values determined by fs-LA show a similar overall range for all Fe isotope analyses ($\delta^{56}Fe_{Mt} = +0.20$‰ to $+1.22$‰), and for averages of multiple analyses within a given area (0.35‰ to 1.13‰; Table EA3, Figs. 3, EA1 and EA3). Because the errors associated with fs-LA analyses are larger than those of the solution-based analyses, almost all samples show no heterogeneity within individual bands beyond analytical error (0.24‰; 2-σ, based on multiple analyses of our magnetite isotope standard). Where it was possible to analyze the same spots on the BIF magnetite bands by both conventional MM and by fs-LA, the results were consistent, confirming that our fs-LA yields stoichiometric isotopic sampling (Figs. 3 and EA4; Beard et al., 2012).

The range in δ^{56}Fe values for magnetite reported here for both MM and fs-LA analyses fall within the range of previously reported values for magnetite from southern West Greenland iron formations (Dauphas et al., 2004; Whitehouse and Fedo, 2007; Fig. 3). However, although some isotopic heterogeneity is seen in our data, the range in δ^{56}Fe values is almost an order-of-magnitude less than that reported in the SIMS study of Whitehouse and Fedo (2007).

4. Discussion

The main finding of this study is that the Isua BIFs have positive and relatively homogeneous $\delta^{56}Fe_{Mt}$ values as measured at two different spatial scales. Our results significantly expand the observations of Dauphas et al. (2004), which involved a limited number of samples. They also test the proposal that micron-scale Fe isotope heterogeneity exists in the Isua BIFs, as proposed by

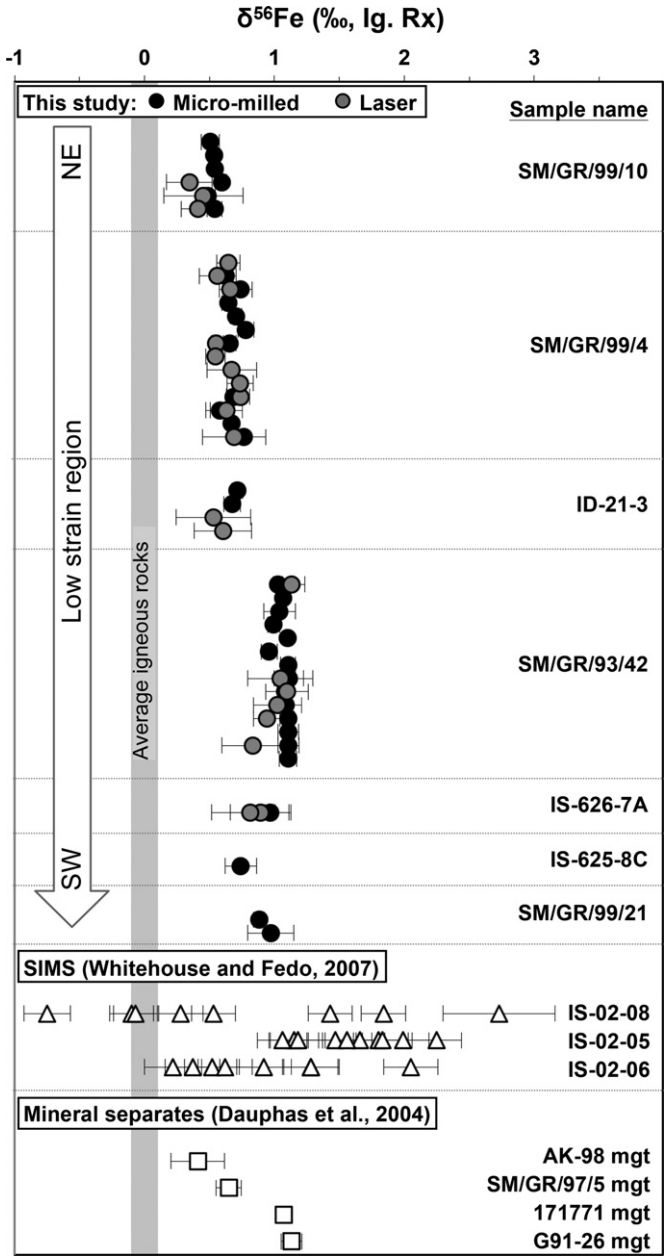

Fig. 3. Fe isotope data for magnetite from southern West Greenland. The plot compares data from magnetites of the Isua Supracrustal Belt [black circles = micromilled, gray circles = laser ablation, from the present study; triangles = SIMS analyses (Whitehouse and Fedo, 2007)], and from Akilia and Innersuartuut [squares = mineral separates (Dauphas et al., 2004)]. Error bars are 2 standard deviations based on multiple analyses from single areas within individual bands [see Electronic Annex Tables EA2 and EA3 for data from the present study; otherwise see Whitehouse and Fedo (2007) and Dauphas et al. (2004)]. Data points for the laser and micro-milled samples that fall on the same horizontal line represent analyses of the same area within a band. The data of Dauphas et al. (2004) and Whitehouse and Fedo (2007) were originally reported relative to the IRMM-014 standard and have been recalculated to plot relative to the igneous rocks standard. The vertical open arrow on the upper left side of the figure indicates the general geographic distribution of samples across the low-strain region of the Isua Supracrustal Belt (see Fig. 1B).

Whitehouse and Fedo (2007). Below the discussion first focuses on the scale of isotopic heterogeneity in the Isua BIFs, which provides insight into the question of metamorphic resetting of the Fe isotope compositions, and the overall Fe budget in the rocks. Then the origin of the high δ^{56}Fe values of magnetite is discussed in terms of the most likely means of Fe oxidation at 3.8 Ga, including a dispersion/reaction model to help explain the production of oxidized Fe that has positive δ^{56}Fe values in the marine setting that likely existed during formation of the Isua rocks. Finally, the implications such compositions have for biogeochemical cycling of Fe at various times on the early Earth are discussed.

4.1. Scale of isotopic heterogeneity

The range of $\delta^{56}Fe_{Mt}$ values reported by Whitehouse and Fedo (2007) is significantly larger than that measured in our study (Fig. 3). The maximum range in δ^{56}Fe values for a single magnetite band that were measured for samples collected by MM was 0.21‰ (sample SM/GR/93/42, Table EA2). Multiple fs-LA analyses were performed in many of these same regions and showed a similarly narrow range of δ^{56}Fe values. Although Whitehouse and Fedo (2007) analyzed different samples than those used in our study, they are from the same geographic areas (see Fig. 1B), and their SIMS data spots are broadly similar in size (~18–25 μm diameter for SIMS vs. 60 μm by 60 μm raster areas for fs-LA). The much larger range in $\delta^{56}Fe_{Mt}$ measured by SIMS (~3‰) is not understood, but for both Fe and O isotope analysis by SIMS there can be analytical artifacts of at least 1‰ in $^{56}Fe/^{54}Fe$ and 2‰ in $^{18}O/^{16}O$, sometimes greater, due to differences in the orientation of the magnetite mineral lattice relative to the primary ion beam (Huberty et al., 2010; Kita et al., 2011).

The majority of $\delta^{56}Fe_{Mt}$ values for bulk samples reported by Dauphas et al. (2004) and bulk or *in situ* analyses from this study fall between +0.7‰ and +1.2‰ (Fig. 3), suggesting that this is the dominant Fe isotope composition for BIF magnetite in southern West Greenland. Moreover, it is argued below that the non-zero δ^{56}Fe values of magnetite in the Isua BIFs, as measured in individual layers, probably reflects Fe isotope compositions attained at low temperatures, prior to regional metamorphism. This interpretation was previously argued by Dauphas et al. (2004) and Whitehouse and Fedo (2007), but it is here expanded to include an assessment of diffusional effects of metamorphism over various spatial scales. The Isua BIFs were subjected to metamorphic temperatures ranging from ~470 to 550 °C in the domain of least strain (Rollinson, 2002, 2003). Iron self-diffusion in magnetite is dependent on temperature and O_2 fugacity (Dieckmann and Schmalzried, 1977; Atkinson et al., 1983), and diffusion coefficients were likely to be greater than 10^{-16} cm^2 s^{-1} at ~500 °C (Atkinson et al., 1983; Dauphas et al., 2007a). Using the standard equation for diffusion length of $L=(4\times D\times t)^{½}$ where D is the diffusion coefficient and t is time, the diffusion length for 1 m.yr. and $D=10^{-16}$ cm^2 s^{-1} is ~1 mm. To diffuse completely over the average length of our MM spots (2 mm) would require ~3 m.yr., and over the average length of our fs-LA spots (~0.06 mm) would require ~3 k.y.; such calculations strongly suggest that the micron-scale Fe isotope heterogeneity observed by Whitehouse and Fedo (2007) is highly unlikely in the Isua rocks, given the long-lived nature of the regional metamorphism.

A metamorphic event that lasted 10 m.yr. would preserve distinct isotopic compositions of magnetite grains over a distance of 3.6 mm. The relative homogeneity of our analyses is therefore not surprising on the scale of a hand sample. Isotopic heterogeneity between magnetite bands would be expected, however, even in the same hand sample, because magnetite bands are separated by quartz bands, which would be an effective barrier to Fe diffusion. In addition, it seems unlikely that large-scale transport of Fe during metamorphism would have occurred, and therefore the average positive $\delta^{56}Fe_{Mt}$ values are probably reflective of the average composition of the BIF samples at low temperatures, prior to regional metamorphism. The scales over which the Fe isotope compositions exhibit homogeneity or

heterogeneity are entirely consistent with the scales of Si isotope homogeneity or heterogeneity from the same Isua metasediments (Heck et al., 2011). In summary, consideration of diffusional rates and spatial scales suggests that any mm- or μm-scale Fe isotope heterogeneity that may have existed during deposition of BIF sediment or during early diagenesis has probably been erased by the effects of regional metamorphism, but the overall average $\delta^{56}Fe_{Mt}$ values are likely to be reflective of those of the original BIF sediment.

4.2. Origin of Fe oxides in the Isua BIFs

Magnetite, the principal Fe phase in the Isua BIFs, is not formed directly during oxidation of $Fe(II)_{aq}$, and a common formation pathway involves reaction of poorly crystalline ferric hydroxides with an Fe(II) component (e.g., Klein, 2005). The high metamorphic grade of the Isua rocks raises the possibility that siderite was a primary precipitate, because metamorphic breakdown of siderite will produce magnetite (e.g., Gallagher et al., 1981). Quantitative breakdown of siderite, however, cannot explain the positive $\delta^{56}Fe$ value, because primary siderite should have negative $\delta^{56}Fe$ values (Wiesli et al., 2004). Instead, a model where magnetite at Isua originally formed in a low-temperature marine environment through reaction of poorly crystalline $Fe(OH)_3$ and $Fe(II)_{aq}$ is preferred here. A number of studies have argued that settling of ferric oxide/hydroxide minerals into an $Fe(II)_{aq}$-rich deep ocean layer can result in surface reactions that convert $Fe(OH)_3$ to magnetite (Tronc et al., 1992; Konhauser et al., 2002; Kappler et al., 2005; Klein, 2005). In addition to abiological formation of magnetite through reaction of $Fe(II)_{aq}$ and $Fe(OH)_3$ (Tronc et al., 1992), magnetite may form through bacterial reduction of $Fe(OH)_3$ (Lovley et al., 1987), and a number of workers have proposed such an origin for magnetite in BIFs (e.g., Konhauser et al., 2002).

Our conceptual model is that the $\delta^{56}Fe$ value of magnetite will be controlled by the Fe isotope composition of aqueous Fe(II), the original $Fe(OH)_3$, and the amount of isotopic exchange that takes place between them in the soft sediment, prior to lithification. Two end-member cases can be defined: (1) complete isotopic equilibrium, where the $\delta^{56}Fe$ value of magnetite reflects the equilibrium fractionation between magnetite and $Fe(II)_{aq}$ and the absolute $\delta^{56}Fe$ value assumed for $Fe(II)_{aq}$; and (2) direct synthesis of magnetite through reaction of $Fe(II)_{aq}$ and $Fe(OH)_3$, but no subsequent isotopic exchange between magnetite and $Fe(II)_{aq}$. In the later case, the Fe isotope composition of magnetite will be controlled by the mixing relation:

$$\delta^{56}Fe_{Mt} = 2/3\delta^{56}Fe_{Fe(OH)3} + 1/3\delta^{56}Fe_{Fe(II)aq} \quad (2)$$

Fig. 4 shows the possible curves of $\delta^{56}Fe$ values for magnetite and $Fe(II)_{aq}$ for these two end-member cases, assuming $\delta^{56}Fe$ values for $Fe(OH)_3$ of 0‰, +1‰, and +2‰ (cf. Fig. 8 of Johnson et al., 2008a). For an isotopic equilibrium model, an equilibrium magnetite–$Fe(II)_{aq}$ fractionation based on combining the $\beta^{56/54}$ values for $Fe(II)_{aq}$ from Rustad et al. (2010) and magnetite from Polyakov et al. (2007) is used, which are the preferred formulations based on agreement between experimental investigations of $Fe(II)_{aq}$–mineral fractionations (Beard et al., 2010). Further, two possible scenarios for equilibrium between magnetite and $Fe(II)_{aq}$ are considered. The first is that equilibration occurred in the water column or shallow sediment during early diagenesis at an assumed temperature of 25 °C. At this temperature, the equilibrium magnetite–$Fe(II)_{aq}$ fractionation is $\Delta^{56}Fe = 2.2‰$ and production of the measured magnetite isotope compositions for the Isua BIFs would require that $Fe(II)_{aq}$ have very low $\delta^{56}Fe$ values between −1.9‰ and −1.1‰ (Fig. 4, upper dashed gray line).

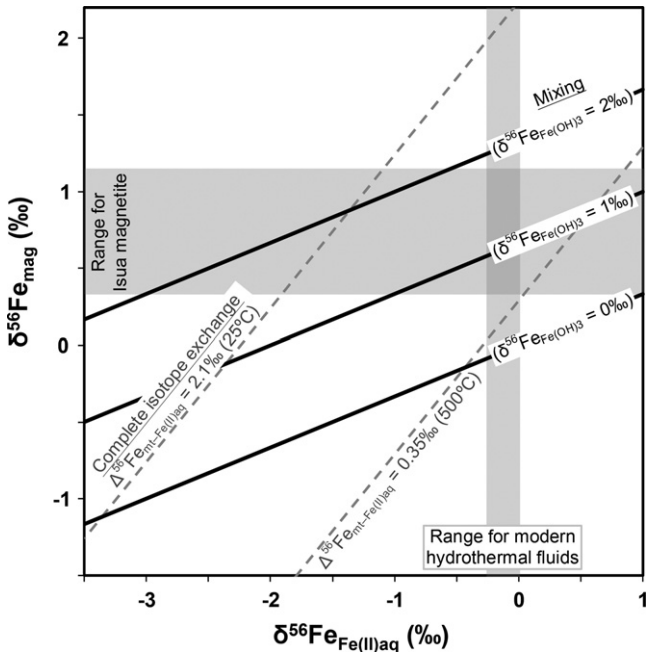

Fig. 4. Theoretical models of possible formation pathways for the Fe isotope compositions of the Isua BIF magnetite. The horizontal and vertical light gray fields represent the ranges of measured Isua magnetite $\delta^{56}Fe$ values and of modern hydrothermal fluid $\delta^{56}Fe$ values, respectively. The dashed gray lines represent models of complete isotope exchange between $Fe(II)_{aq}$ and magnetite either in the water column/shallow sediment (upper line labeled 25 °C) or during regional metamorphism (lower line labeled 500 °C). The $\Delta^{56}Fe$ values are based on the beta factors of (Polyakov et al., 2007; Rustad et al., 2010). The solid black lines represent the formation of magnetite by the mixing of ferric oxides [$Fe(OH)_3$] with $\delta^{56}Fe$ values of 0, +1, or +2‰, and $Fe(II)_{aq}$ in a ratio of 2:1 (see Section 4.2 of the text for details).

The second possibility is that isotopic equilibration occurred by interaction of magnetite with an $Fe(II)_{aq}$-rich fluid during metamorphism at ~500 °C. At this temperature, the equilibrium magnetite–$Fe(II)_{aq}$ fractionation is $\Delta^{56}Fe = 0.3‰$ and production of the measured magnetite isotope compositions would require that $Fe(II)_{aq}$ had high $\delta^{56}Fe$ values between +0.1 and +0.8‰ (Fig. 4, lower dashed gray line). Such low (equilibration in the water column) or high (metamorphic equilibration) $\delta^{56}Fe$ values for $Fe(II)_{aq}$ would require that the Fe is not from hydrothermal sources, which is inconsistent with REE data measured on Isua BIF (Dymek and Klein, 1988; Klein, 2005). The unusual Fe isotope compositions required for $Fe(II)_{aq}$ in the equilibrium model suggests this is not a viable pathway for the Isua magnetite.

The inadequacy of an equilibrium model suggests that the second case is more likely, where synthesis of magnetite occurred through reaction of $Fe(II)_{aq}$ and $Fe(OH)_3$ under conditions where isotopic equilibrium was inhibited. Using Eq. (2), a range of $\delta^{56}Fe$ values between +0.6‰ and +1.65‰ for the primary $Fe(OH)_3$ precipitate can explain the measured $\delta^{56}Fe$ values for magnetite, assuming $Fe(II)_{aq}$ had a $\delta^{56}Fe$ value of 0‰ (Fig. 4, solid black lines). This model can be explored in more detail to understand the oxidation extent that is needed to produce the primary $Fe(OH)_3$ precipitate using a one-dimensional dispersion/reaction model, modified after that of Czaja et al. (2012). As discussed by Czaja et al. (2012), simple approaches for modeling Fe oxidation, such as a Rayleigh model, are not appropriate for the marine environments where BIF deposition occurred, which require accounting for simultaneous input of Fe(II) and removal of Fe(III) oxide precipitates.

Two versions of the dispersion/reaction model were developed, both of which assumed a flux of Fe from the deep ocean, and isotopic fractionation during Fe(II) oxidation: (1) oxidation of

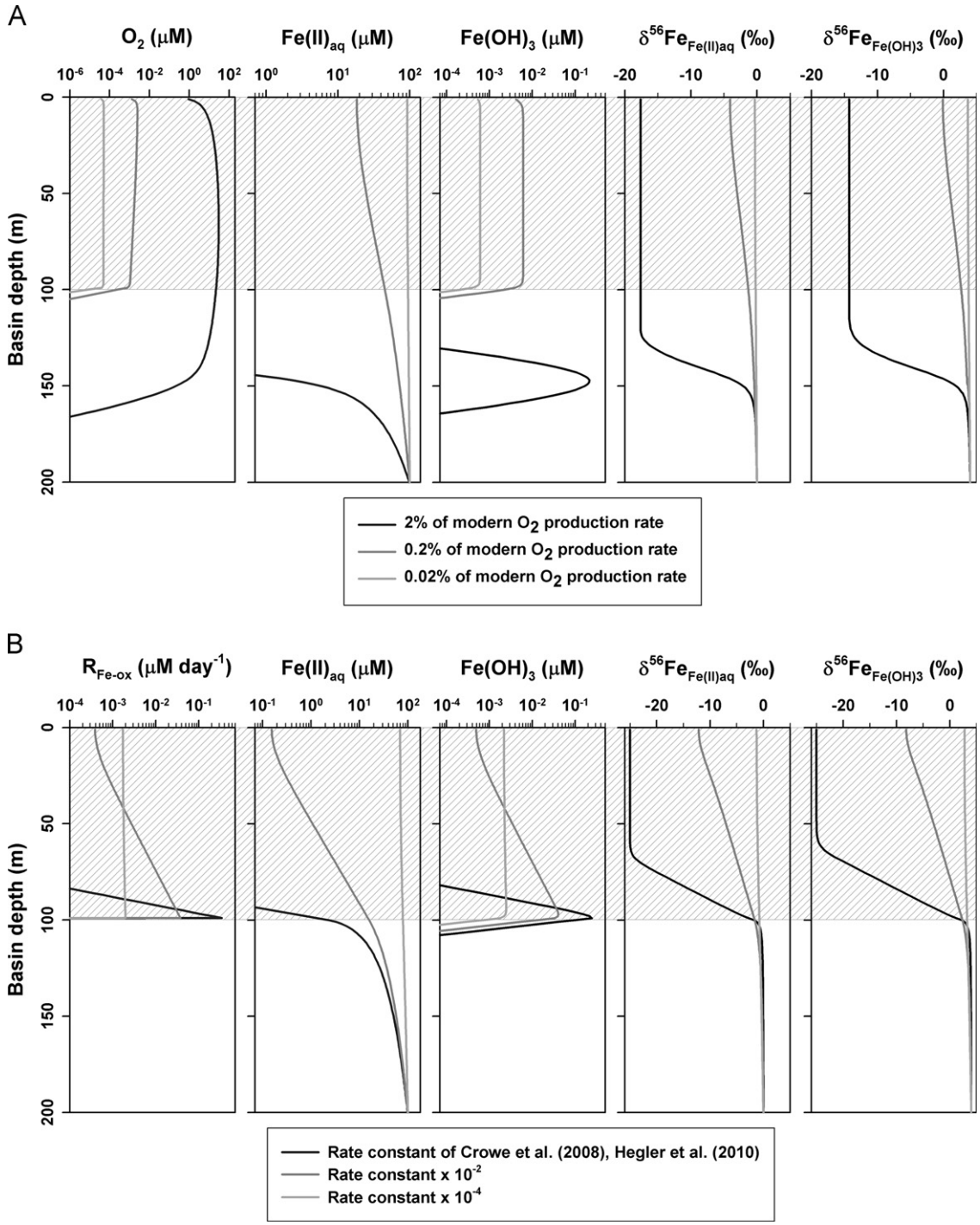

Fig. 5. Representative depth profiles for the dispersion/reaction models. (A) Results from the model that included O_2 production/release in the photic zone and subsequent abiological oxidation of $Fe(II)_{aq}$. (B) Results from the model that included no O_2 production, but $Fe(II)_{aq}$ oxidation by anoxygenic phototrophs in the photic zone. Each set of panels shows the resulting $Fe(II)_{aq}$ and $Fe(OH)_3$ concentrations and $\delta^{56}Fe$ values of these Fe pools. Additionally, A includes depth profiles of O_2 concentration, and B includes profiles of the rates of $Fe(II)_{aq}$ oxidation (R_{Fe-ox}). The hashed areas spanning 0–100 m indicate the depth of the photic zone modeled.

$Fe(II)_{aq}$ by ambient O_2 produced by oxygenic photosynthesis (version 1); and (2) oxidation of $Fe(II)_{aq}$ under anoxic conditions by anoxygenic photosynthetic Fe(II) oxidation (version 2). For simplicity, the same Fe isotope fractionation factors for both oxic and anoxic versions of the model are used. The most recent experimental determination of the fractionation factor between $Fe(II)_{aq}$ and Fe (oxy)hydroxides in a simulated Archean marine solution (including silica saturation) yielded a maximum $\Delta^{56}Fe_{Fe(OH)3\text{-}Fe(II)aq}$ of 4‰, although the fractionation factor can be as low as 2.5‰, depending upon Fe/Si ratios (Wu et al., 2011, 2012). To date, anoxygenic photosynthetic Fe(II) oxidation has been shown to produce an $Fe(OH)_3$–$Fe(II)_{aq}$ fractionation of ~1.5‰ (Croal et al., 2004). It is important to note, however, that these experiments were not performed in solutions similar in composition to the Archean ocean, namely at silica saturation, and recent work has shown that in general the $Fe(OH)_3$–$Fe(II)_{aq}$ fractionation increases in the presence of silica (Wu et al., 2011, 2012). Kappler et al. (2010) measured a $Fe(OH)_3$–$Fe(II)_{aq}$ fractionation of ~3‰ during microbial oxidation of $Fe(II)_{aq}$ coupled to nitrate reduction and argued that the higher fractionation factor relative to that of Croal et al. (2004) reflects

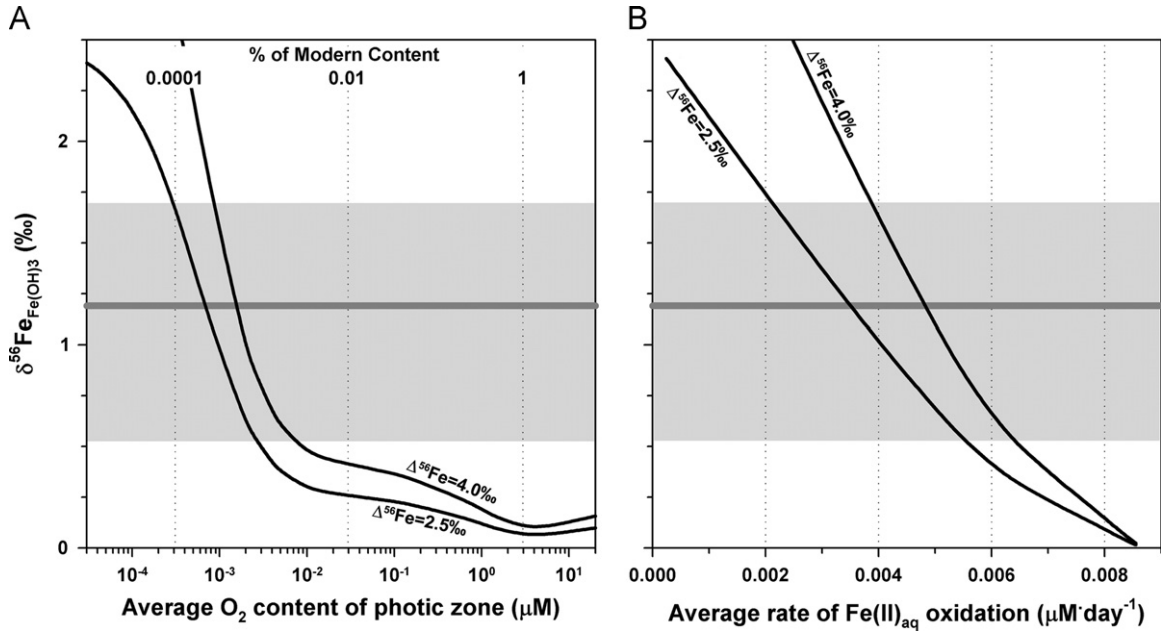

Fig. 6. Summary results of dispersion/reaction modeling of the Isua basin assuming net production of O_2 by oxygenic photosynthesis or Fe oxidation by anoxygenic photosynthetic Fe oxidizers. (A) Resulting average photic zone O_2 concentrations plotted against the weighted average δ^{56}Fe values of the $Fe(OH)_3$ produced when initial rate of O_2 production was varied. (B) Resulting average rates of $Fe(II)_{aq}$ oxidation in the photic zone plotted against the resulting weighted average δ^{56}Fe values of the $Fe(OH)_3$ produced when the rate of anoxygenic Fe(II) oxidation was varied. The two curves in each panel represent the model results for Fe isotope fractionation factors between $Fe(II)_{aq}$ and $Fe(OH)_3$ of $\Delta^{56}Fe_{Fe(OH)3-Fe(II)aq}$=2.5‰ and 4.0‰. The horizontal dark gray line in each panel at δ^{56}Fe=1.19‰ represents the assumed average δ^{56}Fe value for the $Fe(OH)_3$ produced by $Fe(II)_{aq}$ oxidation during Isua BIF deposition. This value was calculated from the average measured δ^{56}Fe value (0.79‰) and the assumption that one-third of the Fe in magnetite (Fe_3O_4) was provided by addition of $Fe(II)_{aq}$ ($\delta^{56}Fe_{Fe(II)aq}$=0‰) to the initial $Fe(OH)_3$ precipitate; thus, $\delta^{56}Fe_{Fe(OH)3}=[\delta^{56}Fe_{Mt}-{}^1/_3(\delta^{56}Fe_{Fe(II)aq})]/{}^2/_3$. The light gray field in each panel shows the range of measured δ^{56}Fe values, also recalculated as above.

attainment of isotopic equilibrium due to oxidation in the periplasm. For version 1 of the dispersion/reaction model, oxidation by ambient O_2, the model is essentially the same as that of Czaja et al. (2012). One difference is that a pH of 7.5 was used in the present study because the Archean atmosphere had higher CO_2 contents, and thus a lower pH ($\leq$7.5) than present seawater (Walker, 1983; Grotzinger and Kasting, 1993; Ohmoto et al., 2004). Use of a pH of 7 would not significantly alter our conclusions. For version 2 of the dispersion/reaction model, the model of Czaja et al. (2012) was modified to exclude O_2 production, replaced by a rate equation for anoxygenic phototrophic Fe(II) oxidizers (Kappler et al., 2005; Crowe et al., 2008; Hegler et al., 2008). Both models were run with a basin depth of 200 m and a photic zone depth of 100 m.

Representative depth profiles for a hypothetical 200 m deep basin modeled under oxic conditions (version 1) are shown in Fig. 5A. These profiles show the steady-state conditions for each of the model outputs at the end of the model run. The initial rate of net O_2 production (or O_2 release) used is 2% of the modern rate of total O_2 production. The modern rate of total O_2 production is based on the rate of modern primary productivity, so the use of 2% of this value at the rate of O_2 release accounts for loss of O_2 by remineralization of organic matter and reaction with other reduced species (Czaja et al., 2012). Under these conditions, $Fe(II)_{aq}$ is oxidized well below the base of the photic zone, which leads to complete oxidation of upwelling $Fe(II)_{aq}$, as well as accumulation of significant O_2 in the photic zone ($\sim$20 μM on average; Fig. 5A). A decrease in the rate of oxygen release over an order of magnitude is required to produce incomplete $Fe(II)_{aq}$ oxidation, which in turn results in a major reduction in the amount of $Fe(OH)_3$ produced (Fig. 5A). From these profiles, the weighted average δ^{56}Fe values for $Fe(OH)_3$ precipitates and average O_2 concentrations in the photic zone can be calculated. It is necessary to decrease the rate of O_2 release by more than an order of magnitude from our initial value of 2% of the modern rate in order to produce $Fe(OH)_3$ precipitates that have an average δ^{56}Fe value of 1.19‰ (the calculated average δ^{56}Fe value of the primary precipitate based on Eq. (3), above in this section; see also Fig. 6 and caption). Doing so reduces the resulting concentration of O_2 in the photic zone from $\sim$20 μM to $\sim$1–2 nM (or $<$0.001% of the modern concentration of O_2; Fig. 6A). The oxic model therefore suggests that if oxygenic photosynthesis was responsible for Fe(II) oxidation at 3.8 Ga in the Isua basin, then the phototrophs were either much less efficient than modern analogs in producing O_2 or the reducing capacity of the ancient Earth was sufficient to keep O_2 contents as very low levels. Without independent evidence for the metabolic rates of the organisms that were present, or nutrient availability in the Isua basin, the first possibility is difficult to assess. Oxygenic photosynthesis, however, is a very energetically favorable reaction, which suggests that organisms capable of performing this metabolism would have proliferated rapidly after they evolved. This leaves the possibility that all of the O_2 produced was scrubbed from the atmosphere/hydrosphere by reduced species. The Early Archean Earth did have a large reducing capacity that could have keep O_2 low, if a source of O_2 existed, but it seems unreasonable that it would take more than 1 billion years for O_2 to appreciably build up in the atmosphere. If this were the case, large quantities of oxidized Fe and other redox sensitive elements should have been deposited throughout the Archean, but such deposits (e.g., Superior-type BIFs) do not appear until much later in the Archean and into the Proterozoic (Klein, 2005; and Section 4.3).

Another possibility is that anoxygenic phototrophs were the mechanism responsible for oxidation of Fe(II). Fig. 5B shows steady-state depth profiles for a 200 m deep basin modeled under anoxic conditions. Using a rate constant for anoxygenic photosynthetic Fe(II) oxidation comparable to that of experimental studies of anoxygenic photosynthetic Fe(II) oxidation, as well as calculated from modern analog environments (0.25 day^{-1}; Kappler et al., 2005; Crowe et al., 2008; Hegler et al., 2008), complete $Fe(II)_{aq}$ oxidation occurs, but if this rate is decreased by

Table 1
Comparison of Isua and Hamersley banded iron formations.

Properties	Location	Age (Ga)	$\delta^{56}Fe_{Mt}$[a] (‰)		Fe[b] (moles)	Fe conc.[b] (moles m^{-2})
			Average	Range		
Isua	Greenland	3.8	0.79	0.35–1.13	10^{14}	4×10^{11}
Hamersley	Western Australia	2.5	−0.12	−1.19–1.19	10^{18}	2×10^{13}
Transvaal	South Africa	2.5	−0.29	−0.95–1.06	2×10^{18}	2×10^{13}

[a] Isua data from present study. Hamersley and Transvaal data from Johnson et al. (2003), Rouxel et al. (2005), Johnson et al. (2008a), and Steinhoefel et al. (2010).
[b] Isua values based on Fe contents reported by Dymek and Klein (1988) and deposit area and thickness from Nutman et al. (1984). Hamersley values based on average Fe contents reported by Trendall and Blockley (1970) and deposit area and thickness from Trendall (1983). Transvaal values based on Fe contents reported by Klein and Beukes (1992) and deposit area and thickness from Beukes (1983).

a few orders of magnitude, incomplete oxidation occurs and the amount of $Fe(OH)_3$ produced is decreased (Fig. 5B). Calculation of the weighted-average $\delta^{56}Fe$ value of the $Fe(OH)_3$ produced indicates that the rate of oxidation must be decreased by more than two orders of magnitude to attain a value similar to the average $\delta^{56}Fe$ value of the Isua BIF oxide precursor (Fig. 6B). This is reasonable given that the experiments designed to determine the rate of Fe(II) oxidation (Kappler et al., 2005; Hegler et al., 2008) were performed under ideal conditions of light, pH, temperature and nutrients in batch reactors, but in a marine setting, such conditions do not persist. So whereas the maximum rate attained in the Isua basin could have been comparable to that of the experiments, diurnal cycles of light and dark, lower solar luminosity, as well as seasonal cycles of productivity and nutrient availability would have markedly decreased the average rate. Additionally, there is much variability in the rates of Fe oxidation between the various taxa of modern anoxygenic phototrophs (Kappler et al., 2005; Hegler et al., 2008), and ancient anoxygenic phototrophs were likely no less variable. Based on our modeling, as well as independent S isotope evidence for a lack of significant O_2 in the Early Archean environment (Holland, 1984; Farquhar et al., 2000; Mojzsis et al., 2003; Whitehouse et al., 2005), we suggest that anoxygenic photosynthetic Fe(II) oxidation rather than oxygenic photosynthesis was responsible for production of Isua BIF oxides at 3.8 Ga.

4.3. Comparison to younger BIFs and implications for the Early Archean Fe cycle

Although BIFs have figured prominently in discussions on the Fe cycle, the size of the Fe inventories of Archean BIFs varied by many orders of magnitude. The Isua BIFs are relatively small, with an Fe footprint of 4×10^{11} mol km^{-2}, which is a fraction of the size of the large 2.5 Ga BIFs of the Hamersley and Transvaal basins, which have Fe footprints of 2×10^{13} mol km^{-2} each (Table 1). Although it is difficult to estimate Fe deposition rates for these BIFs, if hydrothermal Fe fluxes scale with global heat flow, Fe fluxes during deposition of the Isua BIFs may have been a factor of two higher than those during deposition of the 2.5 Ga BIFs (Jackson and Pollack, 1984). That the Fe footprint of the Isua BIFs are two orders-of-magnitude less than the 2.5 Ga BIFs therefore suggests that the amount of hydrothermal Fe(II) that was oxidized at 3.8 Ga was but a small fraction of that oxidized at 2.5 Ga. Comparison of magnetite Fe isotope data from the 3.8 Ga Isua BIFs with the 2.5 Ga Hamersley and Transvaal BIFs (Fig. 7) supports a model that there was a fundamental difference between the Fe cycles that produced the BIFs in these time periods that reflects different extents of oxidation, as well as microbial diagenesis. Magnetite from the Isua BIFs has an average $\delta^{56}Fe$ value that is positive (~0.8‰) and an overall range that is relatively small (±0.4‰), whereas magnetite in the Hamersley and Transvaal BIFs has an average $\delta^{56}Fe$ value that is slightly negative (~−0.2‰) and a much wider range (±1.2‰; Table 1). The peak in $\delta^{56}Fe_{Mt}$ values for the Hamersley and Transvaal BIFs centered close to 0‰ (Johnson et al., 2003, 2008a; Rouxel et al., 2005; Steinhoefel et al., 2010) has been interpreted to reflect inheritance of $\delta^{56}Fe$ values of $Fe(OH)_3$ that was produced by complete oxidation of $Fe(II)_{aq}$ (Johnson et al., 2008b). Because $\delta^{56}Fe$ values do not scale linearly with O_2 contents or oxidation rate (Fig. 6), the moderately positive $\delta^{56}Fe$ values inferred for Isua Fe(III) oxide precipitates indicates very low ambient O_2 contents and small extents of oxidation.

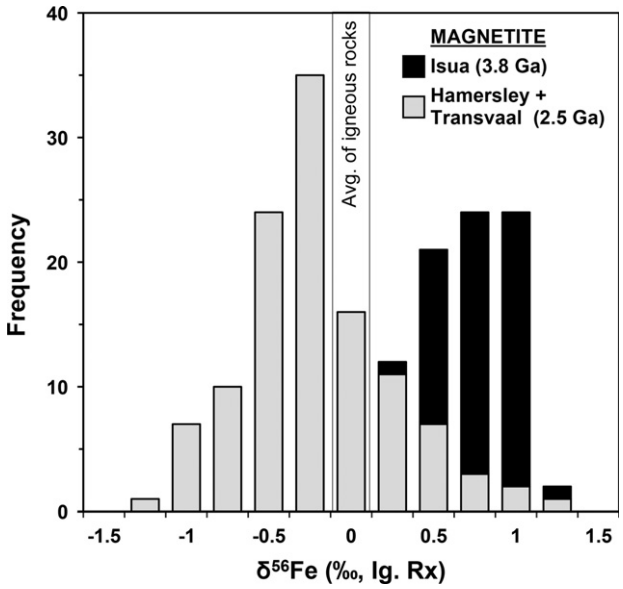

Fig. 7. Comparison of BIF magnetite Fe isotope compositions of the 3.8 Ga Isua Supracrustal Belt and 2.5 Ga Hamersley and Transvaal basins. This comparison suggests a fundamental difference in the Fe cycles that produced the BIFs in these two time periods. The peak in $\delta^{56}Fe_{Mt}$ values for the Hamersley and Transvaal basin BIFs is centered just below 0‰, distinctly lower than the distribution of $\delta^{56}Fe$ values of the Isua BIF. Johnson et al. (2008a) interpret the peak at $\delta^{56}Fe$ ~0‰ for the 2.5 Ga BIFs to reflect the inheritance of the $\delta^{56}Fe$ values of $Fe(OH)_3$ that was produced by complete oxidation of $Fe(II)_{aq}$, whereas Isua $\delta^{56}Fe_{Mt}$ values greater than zero are thought to reflect partial oxidation. Data for Isua BIFs are from the present study and those for the Neoarchean/Paleoproterozoic Hamersley and Transvaal BIFs are from Johnson et al. (2003, 2008a), Rouxel et al. (2005) and Steinhoefel et al. (2010).

An important finding of the current study is demonstration of little Fe isotope heterogeneity in the Isua BIFs, which stands in contrast to the relatively large range in $\delta^{56}Fe$ values for the 2.5 Ga BIFs (Fig. 7). Although the high-grade nature of metamorphism of the Isua BIFs probably homogenized any initial Fe isotope variability at the micron scale, metamorphism is unlikely to have homogenized Fe isotope compositions across magnetite layers, as discussed in Section 4.1. For the 2.5 Ga BIFs, Fe isotope variability exists between individual bands at the millimeter and larger scale

(Johnson et al., 2003,2008a), a feature not observed in the Isua BIFs. Isotopic variability in the 2.5 Ga BIFs has been interpreted to reflect several processes. The $\delta^{56}Fe_{Mt}$ values that are greater than zero likely reflect partial oxidation, whereas those that are less than zero probably reflect interaction with low-δ^{56}Fe $Fe(II)_{aq}$ that was generated by dissimilatory Fe(III) reduction (DIR; Johnson et al., 2008b). Because negative δ^{56}Fe values are not found in the sedimentary record prior to around 2.9 Ga, Johnson et al. (2008b) suggested that DIR did not have a large impact on the marine sedimentary record before that time. Craddock and Dauphas (2011), however, argued based on coupled δ^{56}Fe and δ^{13}C values in metacarbonates from Isua that DIR was present at 3.8 Ga. We hypothesize that although DIR likely existed at the time of deposition of the Isua BIFs, the quantities of Fe(III) produced by anoxygenic photosynthetic iron oxidation were insufficient to support widespread DIR until oxygenic photosynthesis became common (Johnson et al., 2008b), probably starting sometime between about 2.7 and 2.5 Ga.

5. Conclusions

New Fe isotope data from the 3.7 to 3.8 Ga Isua Supracrustal Belt, obtained on mm to μm scales, demonstrate little isotopic variability, in contrast to previous studies that determined an exceptionally wide range of δ^{56}Fe values at the μm scale. δ^{56}Fe values at the hand-sample scale are generally homogeneous within uncertainties, although across the sample suite, δ^{56}Fe values fall in between +0.4‰ and +1.1‰. The lack of fine-scale Fe isotope heterogeneity can be explained by metamorphic re-equilibration within individual bands on the mm to μm scale, but metamorphism cannot explain the Fe isotope homogeneity between bands in the same hand sample. The δ^{56}Fe values that are characteristic of individual hand samples are therefore interpreted to reflect "primary" or "low-temperature" values despite metamorphism.

The positive $\delta^{56}Fe_{Mt}$ values for the Isua BIFs are indicative of partial oxidation of the $Fe(II)_{aq}$ to $Fe(OH)_3$, a precursor to magnetite formation. Partial oxidation and formation of $Fe(OH)_3$ can be a result of atmospheric O_2, or anoxygenic photosynthesis. Oxidation of $Fe(II)_{aq}$ was modeled by a dispersion/reaction model, which accounts for rates of hydrothermal $Fe(II)_{aq}$ input, rates of oxidation, and rates of $Fe(OH)_3$ settling. To explain the positive δ^{56}Fe values inferred for the $Fe(OH)_3$ precursor via oxidation of $Fe(II)_{aq}$ by an oxic pathway requires exceptionally low O_2 contents, $<0.001\%$ of the modern O_2 contents in the photic zone. In contrast, the positive δ^{56}Fe values can be well explained by anoxygenic photosynthetic Fe(II) oxidation using reasonable rates of oxidation. This, in combination with the very low O_2 contents of the oxic pathway model, as well as other geochemical arguments for low atmospheric O_2 levels in the Early Archean (e.g., Holland, 1984), suggests that oxidation of $Fe(II)_{aq}$ most likely occurred by anoxygenic photosynthesis. This in turn supports proposals that anoxygenic photosynthesis evolved prior to oxygenic photosynthesis (e.g., Widdel et al., 1993).

Comparison of Fe isotope data for the 3.8 Ga Isua BIFs and the 2.5 Ga Hamersley Basin and Transvaal Craton BIFs suggests a fundamental difference in the Fe cycles for these time periods. The Hamersley and Transvaal BIFs commonly have large (several per mil) fine-scale Fe isotope heterogeneity on scales ranging from a few millimeters to centimeters. In addition, the fact that the average δ^{56}Fe values of the 2.5 Ga BIFs are near zero, essentially matching that estimated for hydrothermal fluids in the Archean and Proterozoic, indicates that generally complete oxidation of $Fe(II)_{aq}$ occurred. The low-$\delta^{56}Fe_{Mt}$ values suggest interaction with low-δ^{56}Fe $Fe(II)_{aq}$ that was provided by dissimilatory Fe(III) reduction, and the fine-scale isotopic heterogeneity is exactly that predicted by microbial Fe(III) reduction in the soft sediment prior to lithification (Tangalos et al., 2010). In addition, strong support for a major role by microbial Fe(III) reduction in the 2.5 Ga BIFs comes from C and O isotope data (Heimann et al., 2010; Craddock and Dauphas, 2011). There is no clear evidence, however, for microbial Fe(III) reduction in the Isua BIFs based on Fe isotope data on magnetite, as indicated by the lack of negative δ^{56}Fe values and lack of isotopic heterogeneity. This is consistent with the relatively small footprint of the Isua BIFs and positive δ^{56}Fe values, both of which suggest limited production of Fe(III) oxides as compared to the 2.5 Ga BIFs. We suggest that if our proposal is correct that anoxygenic photosynthesis was the most likely pathway for formation of Fe(III) oxide precursors in the Isua BIFs, this pathway produced insufficient Fe(III) oxides and organic carbon to support extensive microbial Fe(III) reduction. Microbial Fe(III) reduction may have only become widespread in marine environments after oxygenic photosynthesis became common, which was able to produce large quantities of Fe(III) and organic carbon.

Acknowledgments

Conventional Fe isotope measurements and whole-rock geochemical analyses were performed by M. Herrick. We also thank J. Fournelle for his assistance with electron microprobe analyses and C. Kelly for use of Merchanteck micro-mill. Finally, we thank Associate Editor T. Harrison and two anonymous reviewers whose comments improved the manuscript. The samples studied here that were originally reported by R. Dymek are part of the extensive BIF collections of C. Klein that were donated to the Department of Geoscience at the University of Wisconsin, Madison by C. Klein. This work was funded by NSF and NASA grants to C.M.J. and B.L.B.

Appendix A. Supporting information

Supplementary data associated with this article can be found in the online version at http://dx.doi.org/10.1016/j.epsl.2012.12.025.

References

Albarède, F., Beard, B.L., Johnson, C.M., 2004. Analytical methods for non-traditional isotopes. In: Rosso, J.J. (Ed.), Geochemistry of Non-Traditional Stable Isotopes. Mineralogical Society of America and Geochemical Society, Washington, DC, pp. 113–152.

Anbar, A.D., Duan, Y., Lyons, T.W., Arnold, G.L., Kendall, B., Creaser, R.A., Kaufman, A.J., Gordon, G.W., Scott, C., Garvin, J., Buick, R., 2007. A whiff of oxygen before the Great Oxidation Event? Science 317, 1903–1906.

André, L., Cardinal, D., Alleman, L.Y., Moorbath, S., 2006. Silicon isotopes in ~3.8 Ga West Greenland rocks as clues to the Eoarchaean supracrustal Si cycle. Earth Planet. Sci. Lett. 245, 162–173.

Appel, P.W.U., Fedo, C.M., Moorbath, S., Myers, J.S., 1998a. Early Archaean Isua supracrustal belt, West Greenland: pilot study of the Isua Multidisciplinary Research Project. Geol. Greenland Surv. Bull. 180, 94–99.

Appel, P.W.U., Fedo, C.M., Moorbath, S., Myers, J.S., 1998b. Recognizable primary volcanic and sedimentary features in a low-strain domain of the highly deformed, oldest known (≈3.7–3.8 Gyr) Greenstone Belt, Isua, West Greenland. Terra Nova 10, 57–62.

Atkinson, A., Odwyer, M.L., Taylor, R.I., 1983. ^{55}Fe diffusion in magnetite crystals at 500 °C and its relevance to oxidation of iron. J. Mater. Sci. 18, 2371–2379.

Beard, B.L., Czaja, A.D., Li, W., Schauer, J.J., Olson, M., Johnson, C.M., 2012. Iron isotope fractionation during femtosecond laser ablation of magnetite determined by aerosol size sorting experiments. Mineral. Mag. 76, 1462.

Beard, B.L., Handler, R.M., Scherer, M.M., Wu, L.L., Czaja, A.D., Heimann, A., Johnson, C.M., 2010. Iron isotope fractionation between aqueous ferrous iron and goethite. Earth Planet. Sci. Lett. 295, 241–250.

Beard, B.L., Johnson, C.M., 1999. High precision iron isotope measurements of terrestrial and lunar materials. Geochim. Cosmochim. Acta 63, 1653–1660.

Beard, B.L., Johnson, C.M., 2004. Inter-mineral Fe isotope variations in mantle-derived rocks and implications for the Fe geochemical cycle. Geochim. Cosmochim. Acta 68, 4727–4743.
Beard, B.L., Johnson, C.M., Skulan, J.L., Nealson, K.H., Cox, L., Sun, H., 2003. Application of Fe isotopes to tracing the geochemical and biological cycling of Fe. Chem. Geol. 195, 87–117.
Beukes, N.J., 1983. Palaeoenvironmental setting of iron-formations in the depositional basin of the Transvaal Supergroup, South Africa. In: Trendall, A.F., Morris, R.C. (Eds.), Iron-Formation: Facts and Problems. Elsevier, Amsterdam, pp. 131–209.
Boak, J.L., Dymek, R.F., 1982. Metamorphism of the ca. 3800 Ma supracrustal rocks at Isua, West Greenland: implications for early Archean crustal evolution. Earth Planet. Sci. Lett. 59, 155–176.
Braterman, P.S., Cairns Smith, A.G., Sloper, R.W., 1983. Photo-oxidation of hydrated Fe^{2+}—significance for banded iron formations. Nature 303, 163–164.
Brocks, J.J., Logan, G.A., Buick, R., Summons, R.E., 1999. Archean molecular fossils and the early rise of eukaryotes. Science 285, 1033–1036.
Cloud Jr., P.E., 1968. Atmospheric and hydrospheric evolution on the primitive earth. Science 160, 729–736.
Craddock, P.R., Dauphas, N., 2011. Iron and carbon isotope evidence for microbial iron respiration throughout the Archean. Earth Planet. Sci. Lett. 303, 121–132.
Croal, L.R., Johnson, C.M., Beard, B.L., Newman, D.K., 2004. Iron isotope fractionation by Fe(II)-oxidizing photoautotrophic bacteria. Geochim. Cosmochim. Acta 68, 1227–1242.
Crowe, S.A., Jones, C., Katsev, S., Magen, C., O'Neill, A.H., Sturm, A., Canfield, D.E., Haffner, G.D., Mucci, A., Sundby, B., Fowle, D.A., 2008. Photoferrotrophs thrive in an Archean Ocean analogue. Proc. Natl. Acad. Sci. USA 105, 15938–15943.
Crowley, J.L., Myers, J.S., Dunning, G.R., 2002. Timing and nature of multiple 3700–3600 Ma tectonic events in intrusive rocks north of the Isua greenstone belt, southern West Greenland. Geol. Soc. Amer. Bull. 114, 1311–1325.
Czaja, A.D., Johnson, C.M., Beard, B.L., Eigenbrode, J.L., Freeman, K.H., Yamaguchi, K.E., 2010. Iron and carbon isotope evidence for ecosystem and environmental diversity in the ~2.7 to 2.5 Ga Hamersley Province, Western Australia. Earth Planet. Sci. Lett. 292, 170–180.
Czaja, A.D., Johnson, C.M., Roden, E.E., Beard, B.L., Voegelin, A.R., Nägler, T.F., Beukes, N.J., Wille, M., 2012. Evidence for free oxygen in the Neoarchean ocean based on coupled iron–molybdenum isotope fractionation. Geochim. Cosmochim. Acta. 86, 118–137.
Dauphas, N., Cates, N.L., Mojzsis, S.J., Busigny, V., 2007a. Identification of chemical sedimentary protoliths using iron isotopes in the >3750 Ma Nuvvuagittuq supracrustal belt, Canada. Earth Planet. Sci. Lett. 254, 358–376.
Dauphas, N., Rouxel, O., 2006. Mass spectrometry and natural variations of iron isotopes. Mass Spectrom. Rev. 25, 515–550.
Dauphas, N., van Zuilen, M., Busigny, V., Lepland, A., Wadhwa, M., Janney, P.E., 2007b. Iron isotope, major and trace element characterization of early Archean supracrustal rocks from SW Greenland: protolith identification and metamorphic overprint. Geochim. Cosmochim. Acta. 71, 4745–4770.
Dauphas, N., van Zuilen, M., Wadhwa, M., Davic, A.M., Marty, B., Janney, P.E., 2004. Clues from Fe isotope variations on the origin of Early Archean BIFs from Greenland. Science 306, 2077–2080.
Dieckmann, R., Schmalzried, H., 1977. Defects and cation diffusion in magnetite (I). Ber. Bunsenges. Phys. Chem. 81, 344–347.
Dymek, R.F., Klein, C., 1988. Chemistry, petrology and origin of banded iron-formation lithologies from the 3800 Ma Isua Supracrustal Belt, West Greenland. Precambrian Res. 39, 247–302.
Eigenbrode, J.L., Freeman, K.H., Summons, R.E., 2008. Methylhopane biomarker hydrocarbons in Hamersley Province sediments provide evidence for Neoarchean aerobiosis. Earth Planet. Sci. Lett. 273, 323–331.
Farquhar, J., Bao, H., Thiemens, M., 2000. Atmospheric influence of Earth's earliest sulfur cycle. Science 289, 756–758.
Fedo, C.M., Myers, J.S., Appel, P.W.U., 2001. Depositional setting and paleogeographic implications of earth's oldest supracrustal rocks, the >3.7 Ga Isua Greenstone belt, West Greenland. Sediment. Geol. 141, 61–77.
Gallagher, P.K., West, K.W., Warne, S.S.J., 1981. Use of the Mössbauer effect to study the thermal decomposition of siderite. Thermochim. Acta 50, 41–47.
Grotzinger, J.P., Kasting, J.F., 1993. New constraints on Precambrian ocean composition. J. Geol. 101, 235–243.
Heck, P.R., Huberty, J.M., Kita, N.T., Ushikubo, T., Kozdon, R., Valley, J.W., 2011. SIMS analyses of silicon and oxygen isotope ratios for quartz from Archean and Paleoproterozoic banded iron formations. Geochim. Cosmochim. Acta 75, 5879–5891.
Hegler, F., Posth, N.R., Jiang, J., Kappler, A., 2008. Physiology of phototrophic iron(II)-oxidizing bacteria: implications for modern and ancient environments. FEMS Microbiol. Ecol. 66, 250–260.
Heijlen, W., Appel, P.W.U., Frezzotti, M.L., Horsewell, A., Touret, J.L.R., 2006. Metamorphic fluid flow in the northeastern part of the 3.8–3.7 Ga Isua Greenstone Belt (SW Greenland): A re-evalution of fluid inclusion evidence for early Archean seafloor-hydrothermal systems. Geochim. Cosmochim. Acta. 70, 3075–3095.
Heimann, A., Johnson, C.M., Beard, B.L., Valley, J.W., Roden, E.E., Spicuzza, M.J., Beukes, N.J., 2010. Fe, C, and O isotope compositions of banded iron formation carbonates demonstrate a major role for dissimilatory iron reduction in ~2.5 Ga marine environments. Earth Planet. Sci. Lett. 294, 8–18.
Herrick, M.J., 2007. Isotopic Studies of the 3.7–3.8 Ga Isua Banded iron Formations Provide Insight into the Early Archean Geochemical Cycles. M.s. Thesis. Department of Geology and Geophysics, University of Wisconsin, Madison, p. 73.
Hoashi, M., Bevacqua, D.C., Otake, T., Watanabe, Y., Hickman, A.H., Utsunomiya, S., Ohmoto, H., 2009. Primary haematite formation in an oxygenated sea 3.46 billion years ago. Nat. Geosci. 2, 301–306.
Holland, H.D., 1984. The Chemical Evolution of the Atmosphere and Oceans. Princeton University Press, Princeton, NJ.
Huberty, J.M., Kita, N.T., Kozdon, R., Heck, P.R., Fournelle, J.H., Spicuzza, M.J., Xu, H.F., Valley, J.W., 2010. Crystal orientation effects in $\delta^{18}O$ for magnetite and hematite by SIMS. Chem. Geol. 276, 269–283.
Jackson, M.J., Pollack, H.N., 1984. On the sensitivity of parameterized convection to the rate of decay of internal heat sources. J. Geophys. Res. 89, 103–108.
Johnson, C.M., Beard, B.L., 2006. Fe isotopes: an emerging technique for understanding modern and ancient biogeochemical cycles. GSA Today 16, 4–10.
Johnson, C.M., Beard, B.L., Beukes, N.J., Klein, C., O'Leary, J.M., 2003. Ancient geochemical cycling in the Earth as inferred from Fe isotope studies of banded iron formations from the Transvaal Craton. Contrib. Mineral. Petrol. 144, 523–547.
Johnson, C.M., Beard, B.L., Klein, C., Beukes, N.J., Roden, E.E., 2008a. Iron isotopes constrain biologic and abiologic processes in banded iron formation genesis. Geochim. Cosmochim. Acta 72, 151–169.
Johnson, C.M., Beard, B.L., Roden, E.E., 2008b. The iron isotope fingerprints of redox and biogeochemical cycling in the modern and ancient Earth. Annu. Rev. Earth Planet. Sci. 36, 457–493.
Kappler, A., Johnson, C.M., Crosby, H.A., Beard, B.L., Newman, D.K., 2010. Evidence for equilibrium iron isotope fractionation by nitrate-reducing iron(II)-oxidizing bacteria. Geochim. Cosmochim. Acta 74, 2826–2842.
Kappler, A., Pasquero, C., Konhauser, K.O., Newman, D.K., 2005. Deposition of banded iron formations by anoxygenic phototrophic Fe(II)-oxidizing bacteria. Geology 33, 865–868.
Kato, Y., Suzuki, K., Nakamura, K., Hickman, A.H., Nedachi, M., Kusakabe, M., Bevacqua, D.C., Ohmoto, H., 2009. Hematite formation by oxygenated groundwater more than 2.76 billion years ago. Earth Planet. Sci. Lett. 278, 40–49.
Kaufman, A.J., Johnston, D.T., Farquhar, J., Masterson, A.L., Lyons, T.W., Bates, S., Anbar, A.D., Arnold, G.L., Garvin, J., Buick, R., 2007. Late Archean biospheric oxygenation and atmospheric evolution. Science 317, 1900–1903.
Kendall, B., Reinhard, C.T., Lyons, T.W., Kaufman, A.J., Poulton, S.W., Anbar, A.D., 2010. Pervasive oxygenation along late Archaean ocean margins. Nat. Geosci. 3, 647–652.
Kita, N.T., Huberty, J.M., Kozdon, R., Beard, B.L., Valley, J.W., 2011. High-precision SIMS oxygen, sulfur and iron stable isotope analyses of geological materials: accuracy, surface topography and crystal orientation. Surf. Interface Anal. 43, 427–431.
Klein, C., 2005. Some Precambrian banded iron-formations (BIFs) from around the world: their age, geologic setting, mineralogy, metamorphism, geochemistry, and origin. Am. Mineral. 90, 1473–1499.
Klein, C., Beukes, N.J., 1992. Time distribution, stratigraphy, and sedimentologic setting, and geochemistry of precambrian iron-formations, The Proterozoic Biosphere, A Multidisciplinary Study. Cambridge University Press, New York, pp. 139–146.
Konhauser, K.O., Amskold, L., Lalonde, S.V., Posth, N.R., Kappler, A., Anbar, A., 2007. Decoupling photochemical Fe(II) oxidation from shallow-water BIF deposition. Earth Planet. Sci. Lett. 258, 87–100.
Konhauser, K.O., Hamade, T., Raiswell, R., Morris, R.C., Ferris, F.G., Southam, G., Canfield, D.E., 2002. Could bacteria have formed the Precambrian banded iron formations? Geology 30, 1079–1082.
Li, W., Johnson, C.M., Beard, B.L., 2012. U–Th–Pb isotope data indicate phanerozoic age for oxidation of the 3.4 Ga Apex Basalt. Earth Planet. Sci. Lett. 319, 197–206.
Lovley, D.R., Stolz, J.F., Nord, G.L., Phillips, E.J.P., 1987. Anaerobic production of magnetite by a dissimilatory iron-reducing microorganism. Nature 330, 252–254.
Mojzsis, S.J., Coath, C.D., Greenwood, J.P., McKeegan, K.D., Harrison, T.M., 2003. Mass-independent isotope effects in Archean (2.5 to 3.8 Ga) sedimentary sulfides determined by ion microprobe analysis. Geochim. Cosmochim. Acta 67, 1635–1658.
Moorbath, S., Onions, R.K., Pankhurs, R.J., 1973. Early Archaean age for Isua iron formation, West Greenland. Nature 245, 138–139.
Myers, J.S., 2001. Protoliths of the 3.8–3.7 Ga Isua greenstone belt, West Greenland. Precambrian Res. 105, 129–141.
Nutman, A.P., 1984. Early Archean crustal evolution of the Isukasia area, southern West Greenland. In: Kröner, A., Greiling, R. (Eds.), Precambrian Tectonics Illustrated. E. Schweizerbart'sche Verlagsbuchhandlung (Nägele u. Obermiller), Germany, Stuttgart, pp. 79–93.
Nutman, A.P., Allaart, J.H., Bridgwater, D., Dimroth, E., Rosing, M., 1984. Stratigraphic and geochemical evidence for the depositional environment of the Early Archean Isua Supracrustal Belt, southern West Greenland. Precambrian Res. 25, 365–396.
Nutman, A.P., Bridgwater, D., 1986. Early Archean Amîtsoq tonalites and granites of the Isukasia area, southern West Greenland: development of the oldest-known sial. Contrib. Mineral. Petrol. 94, 137–148.
Ohmoto, H., Watanabe, Y., Kumazawa, K., 2004. Evidence from massive siderite beds for a CO_2-rich atmosphere before ~1.8 billion years ago. Nature 429, 395–399.

Planavsky, N., Rouxel, O., Bekker, A., Shapiro, R., Fralick, P., Knudsen, A., 2009. Iron-oxidizing microbial ecosystems thrived in late Paleoproterozoic redox-stratified oceans. Earth Planet. Sci. Lett. 286, 230–242.

Polat, A., Frei, R., 2005. The origin of early Archean banded iron formations and of continental crust, Isua, southern West Greenland. Precambrian Res. 138, 151–175.

Polyakov, V.B., Clayton, R.N., Horita, J., Mineev, S.D., 2007. Equilibrium iron isotope fractionation factors of minerals: reevaluation from the data of nuclear inelastic resonant X-ray scattering and Mössbauer spectroscopy. Geochim. Cosmochim. Acta 71, 3833–3846.

Rollinson, H., 2002. The metamorphic history of the Isua Greenstone Belt, West Greenland. In: Fowler, C.M.R., Ebinger, C.J., Hawkesworth, C.J. (Eds.), The Early Earth: Physical, Chemical, and Biological Development. Geological Society, London, pp. 329–350, Special Publications.

Rollinson, H., 2003. Metamorphic history suggested by garnet-growth chronologies in the Isua Greenstone Belt, West Greenland. Precambrian Res. 126, 181–196.

Rosing, M.T., 1999. ^{13}C-depleted carbon microparticles in >3700-Ma sea-floor sedimentary rocks from west Greenland. Science 283, 674–676.

Rosing, M.T., Frei, R., 2004. U-rich Archaean sea-floor sediments from Greenland—indications of >3700 Ma oxygenic photosynthesis. Earth Planet. Sci. Lett. 217, 237–244.

Rosing, M.T., Rose, N.M., Bridgwater, D., Thomsen, H.S., 1996. Earliest part of Earth's stratigraphic record: a reappraisal of the >3.7 Ga Isua (Greenland) supracrustal sequence. Geology 24, 43–46.

Rouxel, O.J., Bekker, A., Edwards, K.J., 2005. Iron isotope constraints on the Archean and Paleoproterozoic ocean redox state. Science 307, 1088–1091.

Rustad, J.R., Casey, W.H., Yin, Q.Z., Bylaska, E.J., Felmy, A.R., Bogatko, S.A., Jackson, V.E., Dixon, D.A., 2010. Isotopic fractionation of Mg^{2+}(aq), Ca^{2+}(aq), and Fe^{2+}(aq) with carbonate minerals. Geochim. Cosmochim. Acta 74, 6301–6323.

Schidlowski, M., Appel, P.W.U., Eichmann, R., Junge, C.E., 1979. Carbon isotope geochemistry of the 3.7×10^9-yr-old Isua sediments, West Greenland: implications for the Archaean carbon and oxygen cycles. Geochim. Cosmochim. Acta 43, 189–199.

Steinhoefel, G., von Blanckenburg, F., Horn, I., Konhauser, K.O., Beukes, N.J., Gutzmer, J., 2010. Deciphering formation processes of banded iron formations from the Transvaal and the Hamersley successions by combined Si and Fe isotope analysis using UV femtosecond laser ablation. Geochim. Cosmochim. Acta. 74, 2677–2696.

Stüeken, E.E., Catling, D.C., Buick, R., 2012. Contributions to late Archaean sulphur cycling by life on land. Nat. Geosci. 5, 722–725.

Tangalos, G.E., Beard, B.L., Johnson, C.M., Alpers, C.N., Shelobolina, E.S., Xu, H., Konishi, H., Roden, E.E., 2010. Microbial production of isotopically light iron(II) in a modern chemically precipitated sediment and implications for isotopic variations in ancient rocks. Geobiology 8, 197–208.

Trendall, A.F., 1983. The Hamersley Basin. In: Trendall, A.F., Morris, R.C. (Eds.), Iron–Formation: Facts and Problems. Elsevier, Amsterdam, pp. 69–129.

Trendall, A.F., 2002. The significance of iron-formation in the Precambrian stratigraphic record. Spec. Publ. Int. Assoc. Sedimentol. 33, 33–66.

Trendall, A.F., Blockley, J.G., 1970. The iron formations of the Precambrian Hamersley Group, Western Australia, GSWA Bulletin 119. Geological Survey of Western Australia, Perth, p. 366.

Tronc, E., Belleville, P., Jolivet, J.P., Livage, J., 1992. Transformation of ferric hydroxide into spinel by Fe(II) adsorption. Langmuir 8, 313–319.

Waldbauer, J.R., Sherman, L.S., Sumner, D.Y., Summons, R.E., 2009. Late Archean molecular fossils from the Transvaal Supergroup record the antiquity of microbial diversity and aerobiosis. Precambrian Res. 169, 28–47.

Walker, J.C.G., 1983. Possible limits on the composition of the Archaean ocean. Nature 302, 518–520.

Whitehouse, M.J., Fedo, C.M., 2007. Microscale heterogeneity of Fe isotopes in >3.71 Ga banded iron formation from the Isua Greenstone Belt, Southwest Greenland. Geology 35, 719–722.

Whitehouse, M.J., Kamber, B.S., Fedo, C.M., Lepland, A., 2005. Integrated Pb- and S-isotope investigation of sulphide minerals from the early Archaean of southwest Greenland. Chem. Geol. 222, 112–131.

Widdel, F., Schnell, S., Heising, S., Ehrenreich, A., Assmus, B., Schink, B., 1993. Ferrous iron oxidation by anoxygenic phototrophic bacteria. Nature 362, 834–836.

Wiesli, R.A., Beard, B.L., Johnson, C.M., 2004. Experimental determination of Fe isotope fractionation between aqueous Fe(II), siderite and "green rust" in abiotic systems. Chem. Geol. 211, 343–362.

Wu, L., Beard, B.L., Roden, E.E., Johnson, C.M., 2011. Stable iron isotope fractionation between aqueous Fe(II) and hydrous ferric oxide. Environ. Sci. Technol. 45, 1847–1852.

Wu, L., Percak-Dennett, E.M., Beard, B.L., Roden, E.E., Johnson, C.M., 2012. Stable iron isotope fractionation between aqueous Fe(II) and model Archean ocean Fe–Si coprecipitates and implications for iron isotope variations in the ancient rock record. Geochim. Cosmochim. Acta. 84, 14–28.

Yamaguchi, K.E., Johnson, C.M., Beard, B.L., Ohmoto, H., 2005. Biogeochemical cycling of iron in the Archean–Paleoproterozoic Earth: constraints from iron isotope variations in sedimentary rocks from the Kaapvaal and Pilbara Cratons. Chem. Geol. 218, 135–169.